Demographics of Close-In *TESS* Exoplanets orbiting FGK Main-sequence Stars

Kaiming Cui, David Armstrong, Andreas Hadjigeorghiou, Marina Lafarga, Ares Osborn, George King, Tim Hallatt, Vedad Kunovac, Lauren Doyle

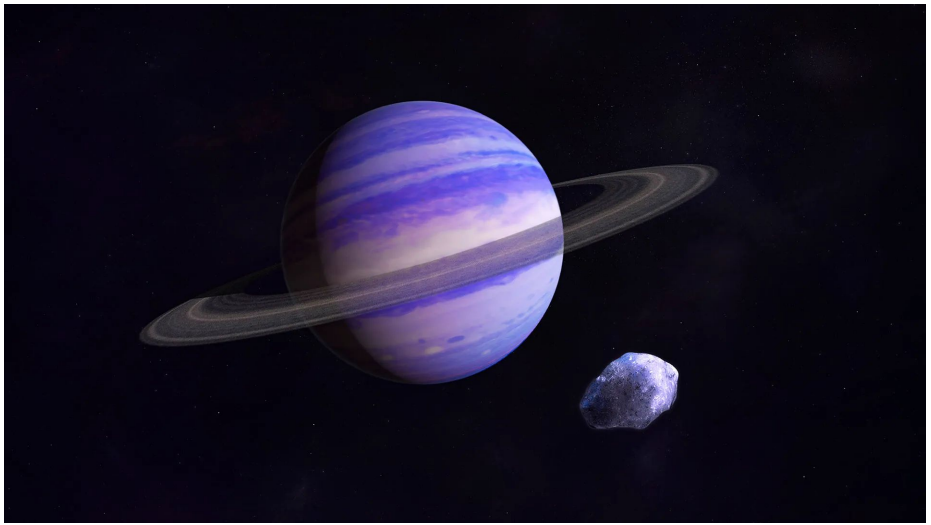
Presentation Outline

- Background
- Science Goal
- Methods
- Results

Exoplanets (Extrasolar Planets)

- Planets that orbit stars other than our sun

- Often categorized by size and orbital period
  - Sub-Earth / Earth-like
  - Super Earth
  - **Sub-Neptunes / Neptunian**
  - Gas Giants / Hot Jupiters

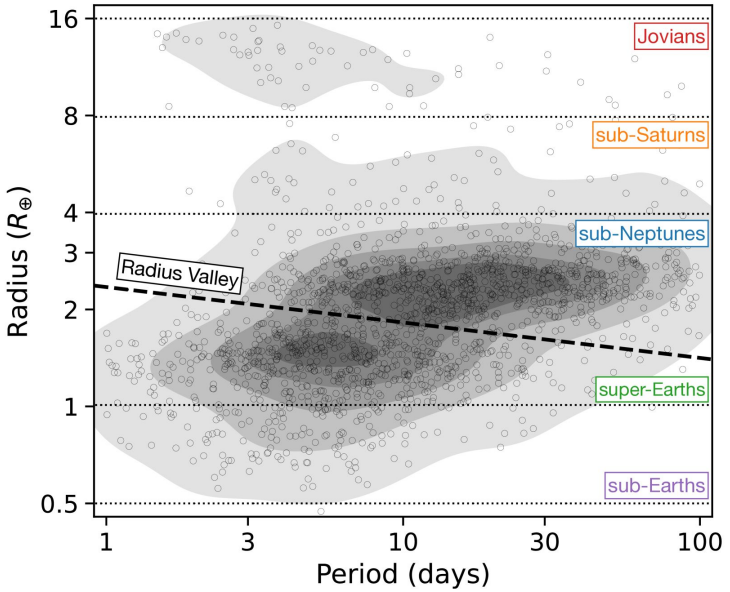


Artist's Rendition of a Gas Giant. Source: *NASA*

Exoplanet Demographics

- Exoplanet demographics is a powerful tool for understanding the formation of planetary systems

- Features in the distribution of known Exoplanets hint at planet formation processes
  - Fulton Radius Gap
  - Hot Jupiters
  - Neptunian Desert



Period-Radius plot of known Exoplanets.
Source: *Gilbert et al. 2025*

Exoplanet Demographics (cont)

- Physical Processes investigated with Exoplanet Demographics
  - Core accretion
  - Disc migration
  - Atmospheric mass loss
    - Stellar irradiation
    - Core cooling

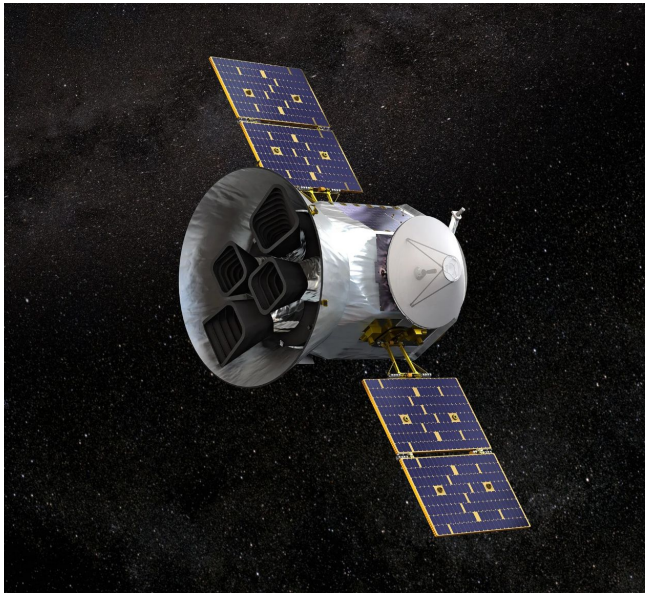
- Some mechanisms are degenerate, distinguishing between them establishes how these processes scale during planet formation

Transiting Exoplanet Survey Satellite (TESS)

- Launched on April 18, 2018

- Uses Transit Method to detect exoplanets around nearby stars
  - > 8000 planet candidates detected
  - > 1000 planets confirmed

- Low resolution, Large FoV



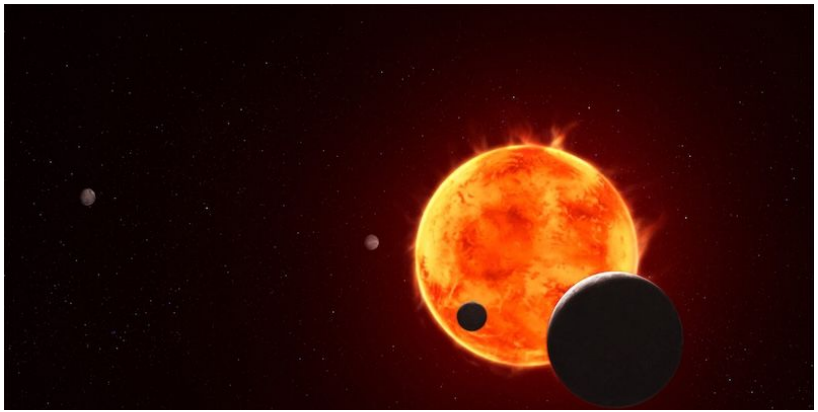
TESS. Source: *NASA*

Science Goals

Objective: Measure planet occurrence rate orbiting FGK-type host stars

- Model the Neptunian Desert among TESS targets

- Search for any trend in occurrence rate space across the Neptunian Desert



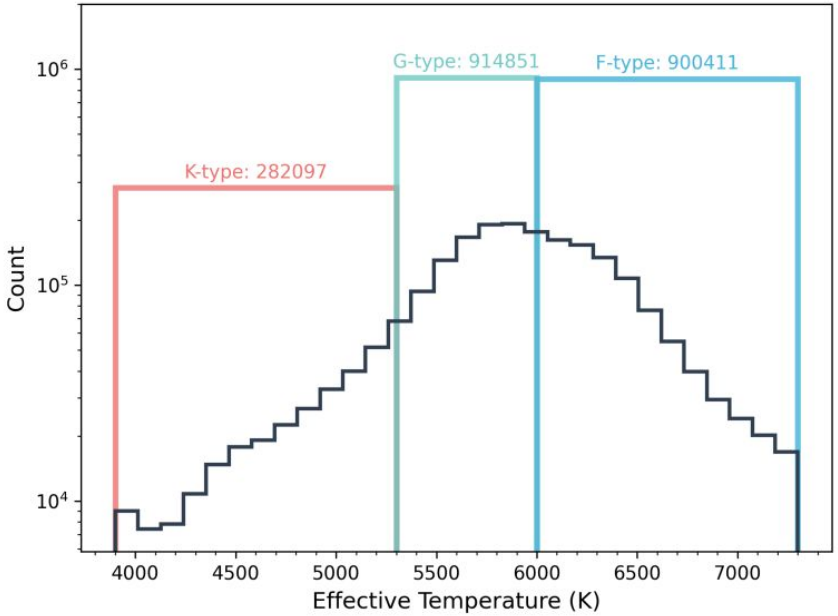
Artist's Rendition of an Exoplanet system. Source: *EarthSky*

Star Selection

- Selected sample from all TESS-SPOC targets

- Selection parameters:
  - TESSmag < 14 mag
  - Parallax/Error > 5
  - Log(g) > 3.5

- Final Sample: 2,097,359 FGK dwarfs

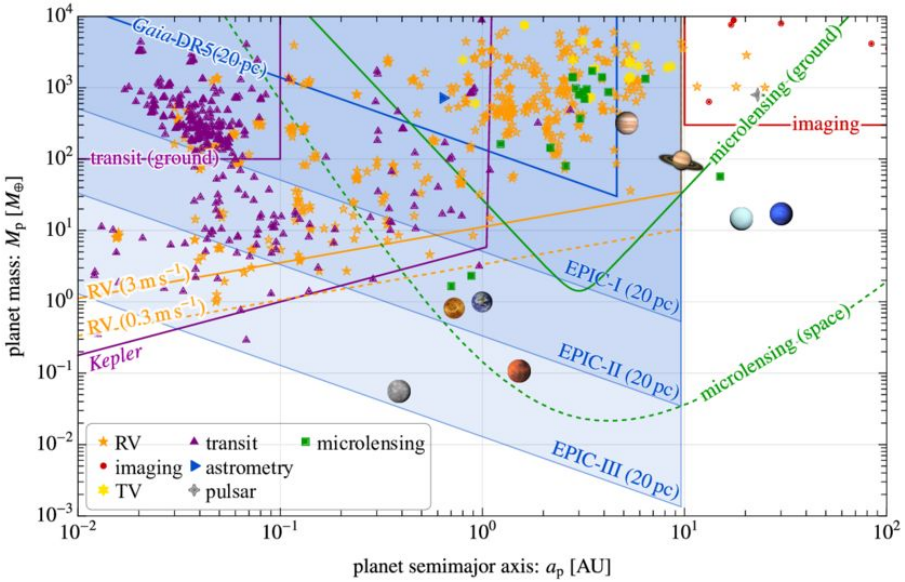


Histogram of selected stars. Source: *K. Cui et al 2026*

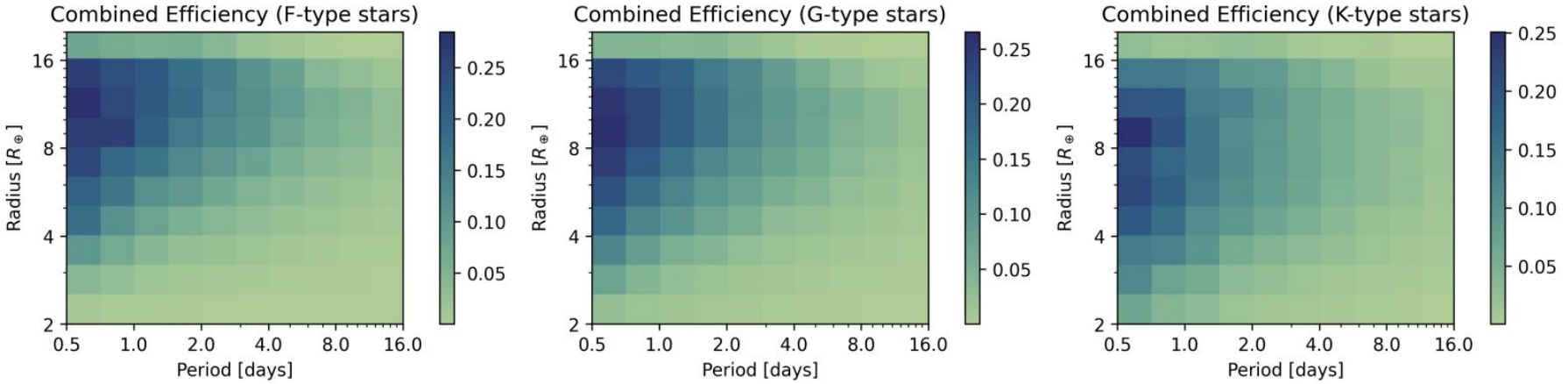
Completeness Estimate

- Accounted for several parameters that may affect sensitivity:
  - Observational Bias
  - Detection Efficiency of Pipeline
  - False Positive Completeness
  - Signal-to-Noise Completeness

- Estimated for each class of star in sample: F,G,K



Detection Sensitivity of various methods and missions. Source: *Galanis et al. 2023*



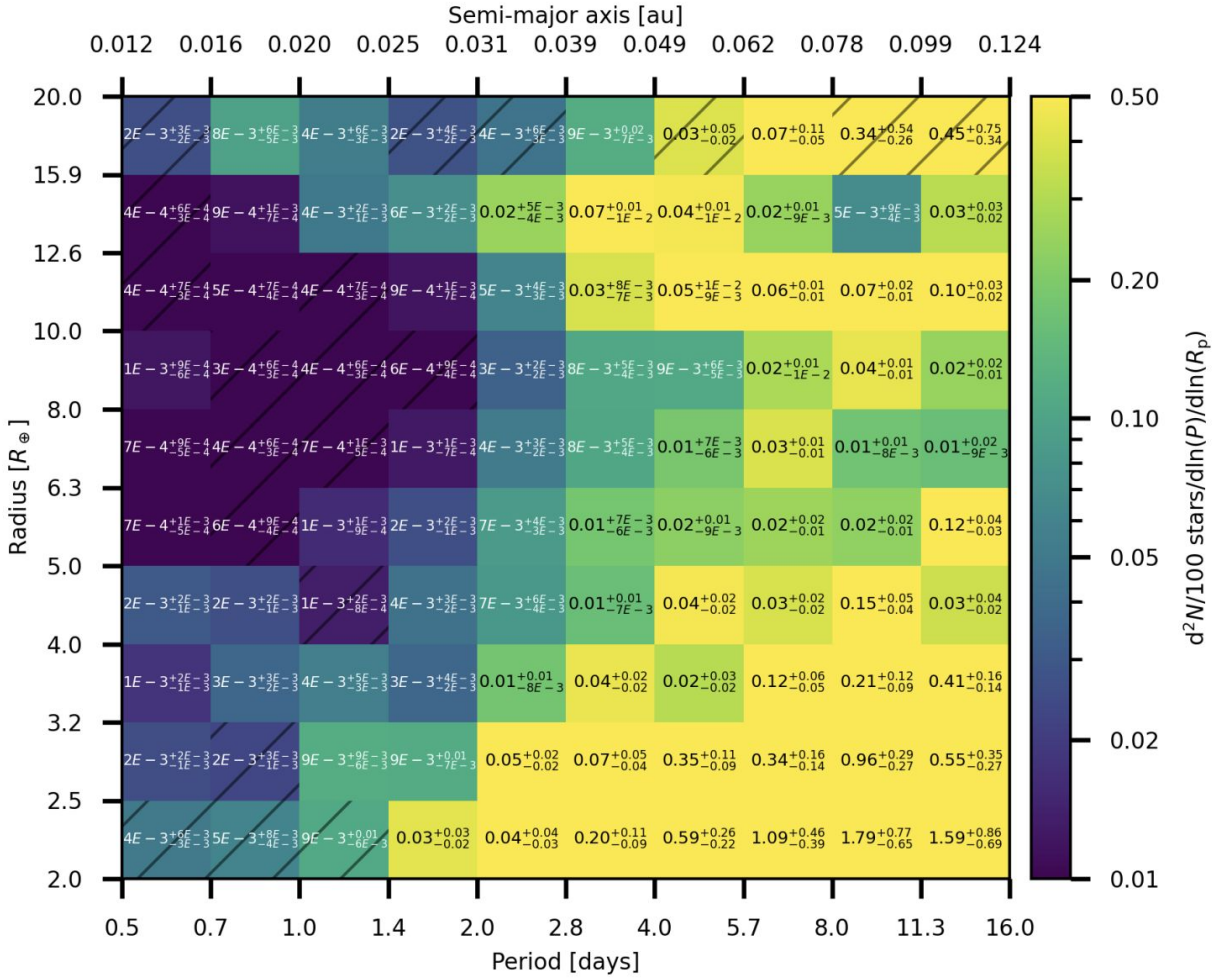
Detection Efficiency of FGK-type stars (TESS detection). Source: *K. Cui et al. 2026*

Occurrence Rate Estimation

- Estimated Occurrence Rate using *Inverse Detection Efficiency Method*
  - Each detection is weighted by the inverse of its detection efficiency

- Example: E (P, r) = 0.5
  - Weight Coefficient: C = 1 / 0.5 = 2
  - Detection accounts for 2 real planets

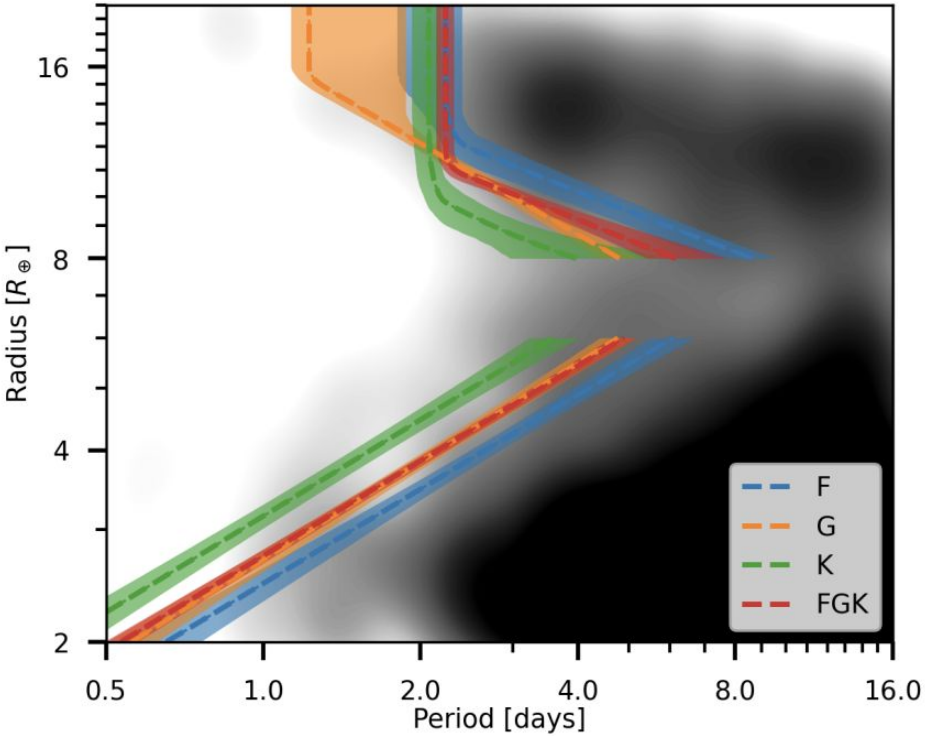
- Creates a 2D-map of Occurrence Rate Density


Semi-major axis [au]
0.012
0.016
0.020
0.025
0.031
0.039
0.049
0.062
0.078
0.099
0.124
Radius [$R_\oplus$]
20.0
15.9
12.6
10.0
8.0
6.3
5.0
4.0
3.2
2.5
2.0
Period [days]
0.5
0.7
1.0
1.4
2.0
2.8
4.0
5.7
8.0
11.3
16.0
$d^2N/100$ stars/dln(P)/dln(R_p)
0.50
0.20
0.10
0.05
0.02
0.01

Modeling the Neptunian Desert

- MCMC method was used to fit bounds of Neptunian Desert

- Fit to the estimated Occurrence Rate, not to detected planet populations
  - Removes observation bias
  - Easier to compare to theoretical models



Upper and Lower bounds of the Neptunian Desert fit to the measured detection efficiency density around FGK-type stars. Source: *K. Cui et al. 2026*

Results

- Bounds of Neptunian Desert were used to determine the average Occurrence Rate across the Desert
- Units of planets/100 stars

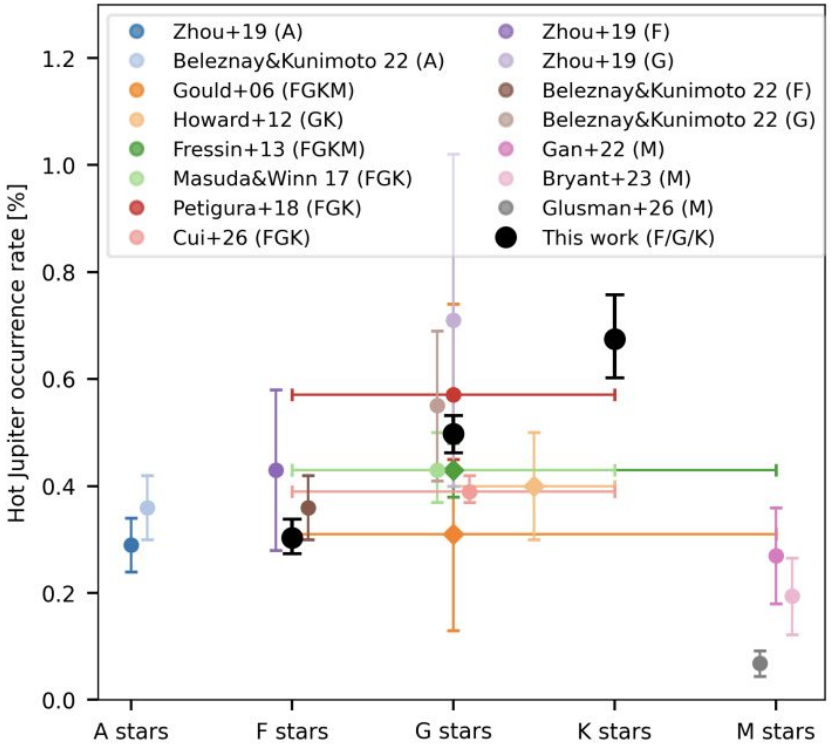
1. “First, the Desert is genuinely empty”
2. Upper bound more spectral dependent than lower bound
3. K-type stars run backwards; emptier for smaller radii

Sample	Upper desert $8–20\ R_\oplus$	P_b (d)	Middle desert $6–8\ R_\oplus$	Lower desert $2–6\ R_\oplus$	Total $2–20\ R_\oplus$
F	$0.0105^{+0.0053}_{-0.0047}$	$4.38^{+8.74}_{-2.58}$	$0.0118^{+0.0445}_{-0.0104}$	$0.0467^{+0.0014}_{-0.0013}$	$0.069^{+0.045}_{-0.011}$
G	$0.0086^{+0.0116}_{-0.0045}$	$6.48^{+5.49}_{-2.39}$	$0.0384^{+0.0448}_{-0.0217}$	$0.0464^{+0.0009}_{-0.0010}$	$0.093^{+0.046}_{-0.022}$
K	$0.0520^{+0.0251}_{-0.0200}$	$4.24^{+0.72}_{-0.48}$	$0.0573^{+0.0221}_{-0.0173}$	$0.0404^{+0.0016}_{-0.0016}$	$0.150^{+0.033}_{-0.026}$
FGK	$0.0305^{+0.0072}_{-0.0069}$	$4.27^{+0.69}_{-0.61}$	$0.0190^{+0.0066}_{-0.0056}$	$0.0457^{+0.0007}_{-0.0008}$	$0.095^{+0.010}_{-0.009}$
FGK†	—	—	—	—	0.08 ± 0.01

Bonus: Hot Jupiters!

- Occurrence Rate increases with decreasing stellar size (FGK-type stars)

- Hot Jupiter Occurrence appears to peak at K-type, not Sun-like



Measured Occurrence Rate of Hot Jupiters across many works.
Source: *K. Cui et al. 2026*

Future Prospects

- More sectors of TESS data = more accurate measurements of Detection Efficiency Density

- Extending Radius Range < 2 Earth Radii can examine small Sub-Neptunes and Fulton Radius Valley

- Incorporating Stellar metallicity and temperature can examine the joint-dependence of other stellar parameters

- Neptunian Desert bounds can be compared to theoretical models of mechanisms present during planet formation

Conclusions

This work built Occurrence Rate maps of Jovian Exoplanets around TESS-detected FGK-type stars

These maps were used to measure the total Occurrence Rate of Neptunian exoplanets, and their Occurrence Rate within the Neptunian Desert

This work measured the Occurrence Rate of Hot Jupiters around FG-type stars, and was the first measurement of Hot Jupiters orbiting K-type stars